

B. TECH PROJECT REPORT

On

**Past and future mass balance-climate
behaviour of Chhota Shigri Glacier(western
Himalaya) using surface energy balance
approach**

BY

ADITYA SINGH, ROHAN AGARWAL



**DISCIPLINE OF CIVIL ENGINEERING
INDIAN INSTITUTE OF TECHNOLOGY INDORE
DECEMBER 2019**

Past and future mass balance-climate
behaviour of Chhota Shigri Glacier(western
Himalaya) using surface energy balance
approach

A PROJECT REPORT

*Submitted in partial fulfillment of the
requirements for the award of the degrees*

of
BACHELOR OF TECHNOLOGY
in

CIVIL ENGINEERING

Submitted by :
ADITYA SINGH, ROHAN AGARWAL

Guided by :
MOHD. FAROOQ AZAM
Assistant Professor
Discipline of Civil Engineering



INDIAN INSTITUTE OF TECHNOLOGY INDORE
DECEMBER 2019

This page is intentionally left blank.

CANDIDATE'S DECLARATION

We hereby declare that the project entitled **Past and future mass balance-climate behaviour of Chhota Shigri Glacier(western Himalaya) using surface energy balance approach** submitted in partial fulfillment for the award of the degree of Bachelor of Technology in Civil Engineering completed under the supervision of **Mohd. Farooq Azam, Assistant Professor, Discipline of Civil Engineering** IIT Indore is an authentic work.

Further, I/we declare that I/we have not submitted this work for the award of any other degree elsewhere.

Signature and name of the student(s) with date

CERTIFICATE by BTP Guide

It is certified that the above statement made by the students is correct to the best of my/our knowledge.

Signature of BTP Guide with dates and their designation

This page is intentionally left blank.

PREFACE

This report on “Past and future mass balance-climate behaviour of Chhota Shigri Glacier(western Himalaya) using surface energy balance approach” is prepared under the guidance of Mohd.Farooq Azam. In this report, we are trying to understand the basic idea of mass balance of the glaciers. The report includes the basic idea and concept behind the model and the results showing the trend followed by the mass balance. All the glacier dynamics are studied, field and model data have been compared and finally used for generating the mass balance.

We have tried to incorporate everything required to understand the modelling of a glacier and to predict the future mass balance of any glacier in a lucid manner.

ADITYA SINGH, ROHAN AGARWAL

B. Tech. IV Year

Discipline of Civil Engineering

IIT Indore

This page is intentionally left blank.

ACKNOWLEDGEMENT

We wish to thank Mohd. Farooq Azam for his kind support and valuable guidance. It is his help and support, due to which we became able to complete the model and technical report. We have to express our appreciation to the guide for sharing his pearls of wisdom with us during the course of this research. Without his support this project would have been a distant reality.

We are thankful to our family who were always there and supported us unconditionally and also to our friends who were there to cheer us up anytime we needed them. We would also like to thank the Institute and the Discipline of Civil Engineering for providing us with the opportunity to work on this project. A special thanks to our teaching assistant Ms. Smriti Shrivastava who was always ready to help us no matter how big or small our problem was.

ADITYA SINGH, ROHAN AGARWAL

B. Tech. IV Year

Discipline of Civil Engineering

IIT Indore

This page is intentionally left blank.

ABSTRACT

Chhota Shigri glacier is located in Lahaul and Spiti Valley, Himachal Pradesh, India. Himalayan glaciers are of particular interest in terms of future water supply, melts and rising water level. With very scant knowledge about the glaciers in the Himalayan region owing to its difficult terrain, this study provides an insight into better understanding these glaciers. Daily Mass balance for the glacier has been investigated for the period from January 1979 to April 2019. An average mass balance of -0.55 ± 0.56 (*meter water equivalent year⁻¹*) is observed for the period from 1980-2018. ERA 5 reanalysis data has been used for all variables. Site data available from two Automatic Weather Stations (*AWS's*) on the glacier for the period from 2009 to 2013 are used to improve the ERA 5 data output. Energy balance approach is deployed to calculate the mass balance. It takes into account accumulation in the form of solid precipitation and ablation in the form of various energy fluxes namely Latent heat flux, Sensible heat flux, Shortwave radiation, and Longwave radiation. CMIP5 along with CNRM-CM5 model has been used for the prediction of future mass balance till the year 2100 for RCP4.5 and RCP8.5. Results indicate increase in the amount of melt and mass balance value decreases as we increase the RCP from 4.5 to 8.5.

This page is intentionally left blank.

TABLE OF CONTENT

Candidate's Declaration
Certificate by BTP Guide
Preface
Acknowledgement
Abstract
List of Figures
List of Tables

Contents

1	Introduction	17
1.1	The Himalayas	17
1.2	Himalayan Glaciers	17
1.3	Glacier Mass Balance	18
1.3.1	Mass Balance	18
1.3.2	Accumulation Zone	18
1.3.3	Ablation Zone	19
1.3.4	Equilibrium Line Altitude	19
1.4	Surface Energy Balance	20
1.4.1	Short-wave Radiation	21
1.4.2	Long-wave Radiation	21
1.4.3	Sensible Heat Flux	21
1.4.4	Latent Heat Flux	21
2	Study Area	22
3	Methodology	24
3.1	Data Acquisition	24
3.1.1	ERA 5	24
3.1.2	Automatic Weather Station	25
3.2	Data Analysis	25
3.2.1	Bias correction	25
4	Mass Balance Model	31
4.1	Glacier Wide Mass Balance	31
4.2	Point Mass Balance	31
4.2.1	Accumulation	31
4.2.2	Ablation	31
4.3	Melt	32
4.3.1	Latent and Sensible Heat Flux	32
4.3.2	Density of Air	32
4.3.3	Surface Temperature	33
4.4	Refreeze Rate	33
4.5	Sublimation and Re-sublimation	33

5	Future Mass Balance	34
6	Results and Discussion	36
6.1	Annual Mass Balance	36
6.1.1	Annual hydrologic mass balance since 1980	36
6.1.2	Seasonal Mass Balance	37
6.2	Model performance	38
6.3	Mass Balance as a function of Altitude	39
6.4	Future Mass Balance	41
7	Conclusion	42

References

List of Tables

1	Geographical and topographical characteristics of Chhota Shigri glacier	24
2	Measurement specification for Automatic Weather Station on Chhota Shigri	26
3	Table showing comparison of modelled mass balance with available mass balances ($mw.e.a^{-1}$)	38

List of Figures

1	Glacier terminologies[8]	18
2	An introduction to glacier mass balance [8].	19
3	Equilibrium Line Altitude[8]	20
4	Surface Energy Balance	20
5	Contour Map of Chhota Shigri glacier showing 50 m elevation bands	22
6	Location map of Chhota Shigri glacier and its surroundings.	23
7	Hypsometry of Chhota Shigri glacier showing 50 m elevation bands	23
8	Bias Correction	26
9	Bias Correction of Net Shortwave	28
10	Bias Correction of Precipitation	29
11	Bias Correction of Surface Temperature	30
12	Bias Correction of Relative Humidity	30
13	Annual hydrologic mass balance since 1980	36
14	Seasonal Mass Balance	37
15	Mass Balance comparison with field data	38
16	Mass Balance comparison with geodetic data	39
17	Mass Balance vs elevation 2010-2017	40
18	Mass Balance for RCP 4.5 and 8.5 year 2007-2100	41

This page is intentionally left blank.

1 Introduction

1.1 The Himalayas

The great ranges of Central Asia contain one of the largest deposits of ice and snow in the world after the polar region. The Hindu Kush Himalaya (HKH) region comprising of the Karakoram, Hindu-Kush and the Himalaya has a total glacierized area of 59000 km^2 (total glacierized area of the world is $540,000 \text{ km}^2$) [18]. Commonly known as the “**Water tower of Asia**” the HKH feeds ten major rivers that provide water for almost two billion people across Asia [38], in addition to supporting energy production, providing food and a wide range of other ecosystem services.

The Himalaya also known as the Earth’s “**Third Pole**” currently harbors around 600 billion tons of ice. The Himalaya are home to more than 12,000 glaciers [29], spanning an area of about $33,000 \text{ km}^2$ [36], storing approximately 12000 km^3 of freshwater. Lifted by the subduction of the Indian Tectonic plate under the Eurasian Plate, the Himalayas have many of the world’s highest peaks including the highest Mount Everest (8848 m). Some of the major glaciers in the Himalayan region are the Gangotri glaciers, Yamnotri glaciers, Zemu glacier, Siachen glacier, Khumbu glaciers and more. The Himalaya have a momentous impact on the lives of people who live near them.

1.2 Himalayan Glaciers

The Himalayan Glaciers play a crucial but erratic role in the water supply of Asia’s main river basins. Glaciers in the Indian Himalaya are the key indicators of regional climate change and water resource to the major rivers like Indus, Ganges and Brahmaputra. Glaciers also contribute to the regional hydrology towards the development and sustainability of downstream population and mountain ecosystems. The degree to which glacier and snowmelt are significant components of the water balance on the large-river-basin scale depends on the glacierized fraction, the hypsometry of the basin, and the pluvial and thermal regimes [28]. Recent studies have shown that glaciers have been shrinking at an accelerated rate since the beginning of the 21st century [12] because of these rapid melt rates formation of massive glacial lakes will take place, with a risk catastrophic glacial lake outburst floods. These floods will also result in loss of life, property, costly infrastructure such as dams, powerhouses, bridges. It is also predicted that this change will lead to considerable changes in the freshwater flow resulting from glacial retreat, with a striking impact on biodiversity, species like the river dolphin which is dependent upon the freshwater from the Himalayas. Species like the snow leopard and the one-horned rhino that needs water for their habitat will be displaced [36]. There is also the risk of natural hazards like landslides *etc.* Although the Himalayan glaciers have a great social and economic impact they have not been studied properly in the past. These glaciers have not been monitored properly and there is only limited knowledge. This lack of knowledge led to some controversial comments like ‘the likelihood of them disappearing by the year 2035 or perhaps sooner is very high if the Earth keeps warming at the current rate’ which was made in the Intergovernmental Panel on Climate Change (IPCC) Fourth Assessment Report [21][17].

Since the Intergovernmental Panel on Climate Change (IPCC) [21] dispute the Himalaya have become the focus of research interest. In recent years, The scientific community has recognized the need to study the Himalayan glacier in greater depths Owing to the lack of data as we go back in time the rate at which the glaciers are melting remains poorly constrained. The IPCC Fifth Assessment Report [40] stated “Several studies of recent glacier velocity change [3] [26] and of the

worldwide present-day sizes of accumulation areas [6] indicate that the world’s glaciers are out of balance with the present climate and thus committed to losing considerable mass in the future, even without further changes in climate”.

Recently many glacier monitoring studies have used remote sensing approaches for the modelling of glaciers (*e.g.* Fujita and Nuimura, 2011[24]; Brun and others, 2017[15]; King and others, 2017[30]). In comparison to the remote sensing approach, there have been fewer in-situ observational studies (*e.g.* Azam and others, 2016[2]; Tshering and Fujita,2016 [43]; Vincent and others, 2016[45]; Sherpa and others, 2017[39]). This is because of the arduous terrain, difficult approach routes, very high altitudes, *etc.* Furthermore, in situ observations are generally limited to lower elevations (*e.g.* Fujita and Nuimura, 2011[24]; Baral and others, 2014[7]; Tshering and Fujita, 2016 [43]; Sherpa and others, 2017[39])

1.3 Glacier Mass Balance

1.3.1 Mass Balance

In the simplest of terms, mass balance refers to the gain and loss of ice from a glacier system. A glacier is a result of how much mass it receives mainly in the form of solid precipitation (snow, snowflakes, etc.) and how much it loses by melting. The concept of mass balance for a glacier is very important for understanding all theories of glacier flow and its behavior.

For better understanding, mass balance can also be referred to as the ‘Health of the glacier’. So, if mass balance is positive it means that glacier is gaining more mass than its losing and glacier will advance, while a negative mass balance would mean that the glacier is losing more mass than it is gaining and hence recede. A glacier can be thought to be in a state of equilibrium if the amount of snow and ice it’s gaining and losing are approximately equal, this would mean that the glacier will neither recede nor advance. For clarification, when we talk about glacier receding or advancing or being in the state of equilibrium we are talking about the position of the snout (the terminus or the toe)(Figure 1). As the glacier has mass it will be in a state continuous flow that means that ice is constantly being displaced from the upper reaches to the lower reaches of the glacier, where it eventually melts.

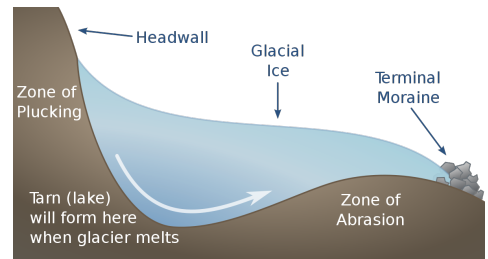


Figure 1: Glacier terminologies[8]

1.3.2 Accumulation Zone

It is through the process of accumulation that the glacier system receives ice and snow. This process of surface accumulation includes ice and snow from direct precipitation, rain, hail, freezing rain, windblown sources, hoar storm, avalanches, etc. Now as the glacier flows, because of the gravitational pull the snow and ice are transferred downslope. Rain along with the refreezing of meltwater percolating through the snowpack may contribute to internal accumulation. Sometimes, freezing of liquid water at the base of the glacier contributes to basal accumulation. Accumulation usually occurs over the entire glacier, but may change with altitude. Warmer air temperatures at lower elevations will also mean precipitation falling as rain and not contributing to accumulation.

Figure 2 gives a brief summary of the glacier system, various input sources as mentioned above account for accumulation, the process of ablation will be discussed in the next section.

1.3.3 Ablation Zone

As discussed in the section above glacier gains mass through the process of accumulation it is through the process of ablation that a glacier loses mass. Ablation represents the ensemble of the various processes that lead to the mass loss of snow and ice. It includes surface melt, sublimation or evaporation at the surface, surface meltwater runoff, avalanching as well as wind-driven transport and sublimation of blowing snow. Glaciers inhabit on an arduous slope may also dry calve, dropping gigantic chunks of ice. Glaciers terminating into water bodies such as the sea or a lake will calve photogenic icebergs. Some other processes of ablation also include subaqueous frontal melt and some melting within the ice and ice beds. As compared to surface melt other form of ablation are not dominant[5], so by implicitly assuming that surface melt is the preeminent form of ablation, most glaciological and hydrological models often use temperature index approaches to model or calculate total ablation.

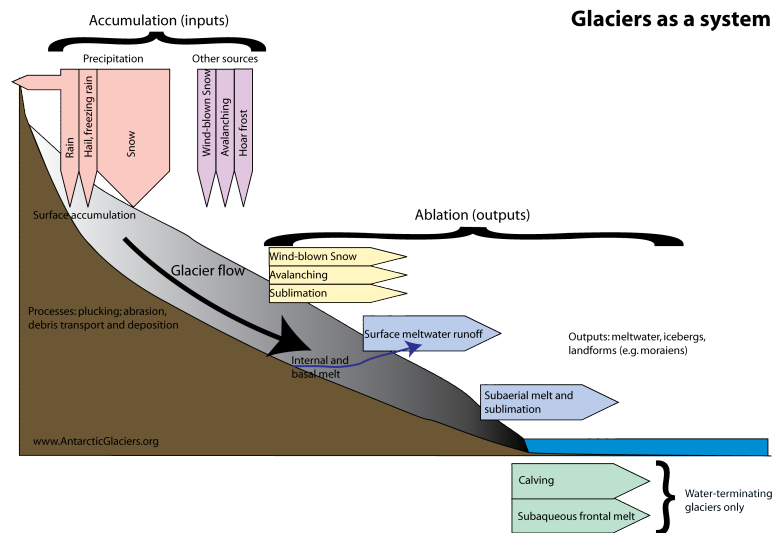


Figure 2: An introduction to glacier mass balance [8].

1.3.4 Equilibrium Line Altitude

As entrenched earlier the zone of ablation is where snow loss exceeds the snowfall, also this lies in the lower region and accumulation zone is the upper region zone where snowfall exceeds the snow loss. The equilibrium line altitude is defined as the elevation at which mass balance is equal, where accumulation of snow is exactly balanced by ablation over a period of a year [27]. So in lay-man terms equilibrium line altitude is the boundary between the ablation and accumulation zone at which mass balance is equal. As equilibrium line is defined in terms of accumulation and ablation, for individual glaciers there is usually a strong correlation between the mass balance and equilibrium line altitude and hence it is closely connected with local climate majorly the air temperatures and precipitation. It serves as an important indicator of glacier response to the change in climate.

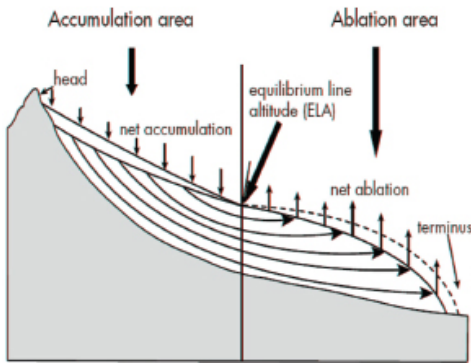


Figure 3: Equilibrium Line Altitude[8]

This has also helped in the reconstruction of former climates and also the prediction of glacier behaviour in the future [9]. The equilibrium line altitude is highly sensitive to perturbations in either the precipitation or the temperature, with rises in response to decrease in the amount of snowfall and/or increasing frequency of positive air temperatures and vice versa [10]. Steady state equilibrium line altitude(ELA) is the value associated with zero annual mass balance for the whole glacier. So the glacier will neither grow nor shrink in the case when the annual ELA coincides with the steady state ELA [9]. However, many glaciers deviate

from the local climate ideas, this is mainly because of regional geographic factors such as shading patterns and the redistribution of snow by wind, also due to avalanches etc.

1.4 Surface Energy Balance

The surface of the glacier is dynamic with the process of accumulation and ablation going on simultaneously. The energy that is exchanged between the surface and the surroundings are mainly due to shortwave radiation, longwave radiation, sensible heat flux, and conductive heat flux. These fluxes help in the melting of the ice at the surface.

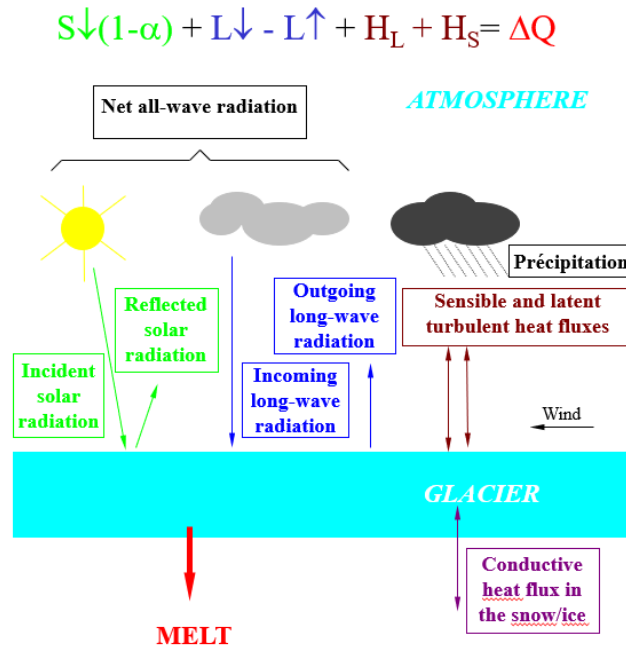


Figure 4: Surface Energy Balance

1.4.1 Short-wave Radiation

Shortwave radiation also known as solar radiation is due to the energy that reaches the surface of the glacier from the sun i.e. in the form of high energy shortwaves. Net shortwave radiation is the sum of downward shortwave radiation (taken as positive) and upward shortwave radiation i.e. reflected from the surface (taken negative). The shortwave radiation is taken in W/m^2 .

1.4.2 Long-wave Radiation

Longwave radiation also known as thermal radiation is due to the energy that reaches the surface of the glacier from the heat of the objects, vegetation, wildlife that are present in the vicinity of the glacier. Net longwave radiation is the sum of downward longwave radiation (taken as positive) and upward longwave radiation i.e. reflected from the surface (taken negative). The longwave radiation is taken in W/m^2 .

Note- When the shortwave radiation is reflected a small part of it $< 5\%$ is neither absorbed nor reflected but is refracted within the top layer of snow and ice and emitted after a few total internal reflections. This results in conductive heat flux which is quite low as compared to shortwave and requires higher mathematics and can be neglected.

1.4.3 Sensible Heat Flux

Sensible heat flux are those fluxes that are caused due to the exchange of heat resulting in the rise of the temperature of the glacial ice and some other macroscopic variables, leaving other macroscopic variables unchanged for example volume or pressure.

1.4.4 Latent Heat Flux

Latent heat flux are those fluxes that are caused due to the exchange of energy resulting in changing of the state of the glacial ice without changing the temperature of the ice. Latent heat from the roots of the word means hidden heat, meaning the heat is used up in the change of the state of the body and is not seen with the change of temperature of the body.

2 Study Area

Chhota Shigri glacier is a valley-type compound glacier (GSI Inventory 2009: Identification No. IN5Q21212159). The direction of the flow of the trunk of the glacier is from south to north. Geographically Chhota Shigri glacier is located between $32^{\circ}11' - 32^{\circ}17' N$ and $77^{\circ}29' - 77^{\circ}33' E$. It lies in the Chandra river basin on the northern ridge of Pir Panjal range in the Lahaul-Spiti valley of Himachal Pradesh, India. A list of geographical and topographical characteristics of Chhota Shigri glacier is given in Table1 [47][37]. In the lower region the slope of the glacier is about 10° to 16° while that in the higher elevations (head of the glacier) is about 40° to 45° [31]. The contour and location of Chhota Shigri glacier on the map can be seen in Figure 5 and Figure 6 respectively.

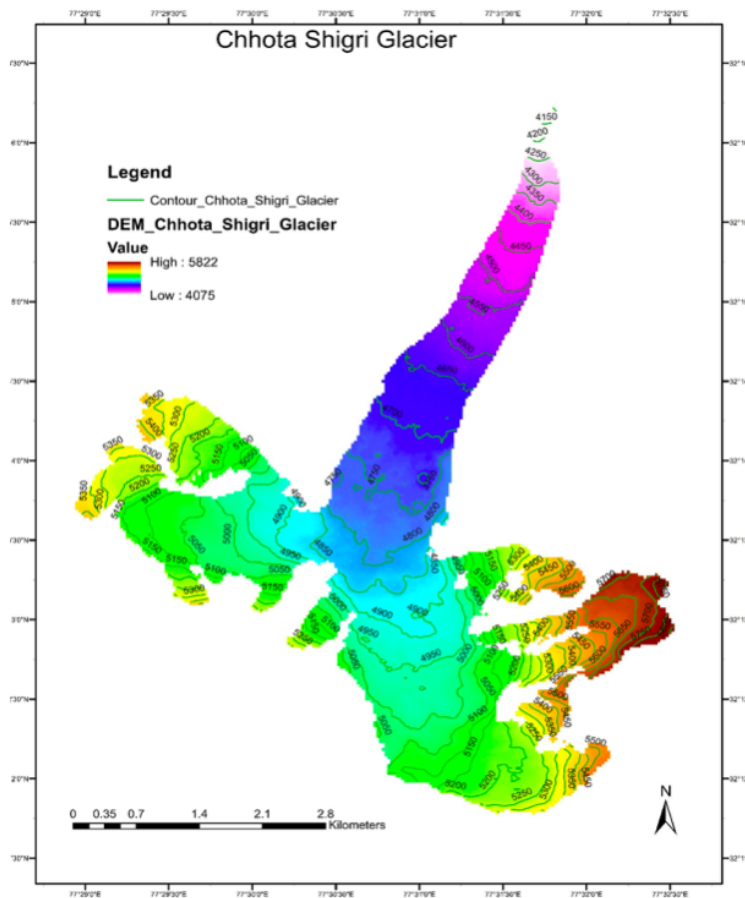


Figure 5: Contour Map of Chhota Shigri glacier showing 50 m elevation bands

and 5500 m respectively. The drainage area of the Chhota Shigri basin is 34.7 km^2 from the location of hydrological station on the proglacial stream at 3900 m a.s.l. , of which 47% is glaciated. The total glaciated area is 16.3 km^2 while the Chhota Shigri glacier covers 15.7 km^2 [47]. Chhota Shigri valley extends 11 km from the Chandra river confluence up to Sara - Umga Pass (4990 m a.s.l.). The main glacier is slightly crescentic with a westerly arch. The lowermost part of the glacier tongue for about 1 km is covered by supraglacial moraines resting mainly on Central Crystalline granites.

The drainage area of the Chhota Shigri basin is 34.7 km^2 from the location of hydrological station on the proglacial stream at 3900 m a.s.l. , of which 47% is glaciated. The total glaciated area is 16.3 km^2 while the Chhota Shigri glacier covers 15.7 km^2 [47]. Chhota Shigri valley extends 11 km from the Chandra river confluence up to Sara - Umga Pass (4990 m a.s.l.). The main glacier is slightly crescentic with a westerly arch. Towards the east of the glacier lies a 28 km long glacier with an area of 131 km^2 , the Bara Shigri glacier, this is the largest glacier of Himachal Pradesh. Mainly two tributary feed the Chhota Shigri glacier one from the east and the other from the west. They both originate from peaks located in the vicinity at around 6000 m

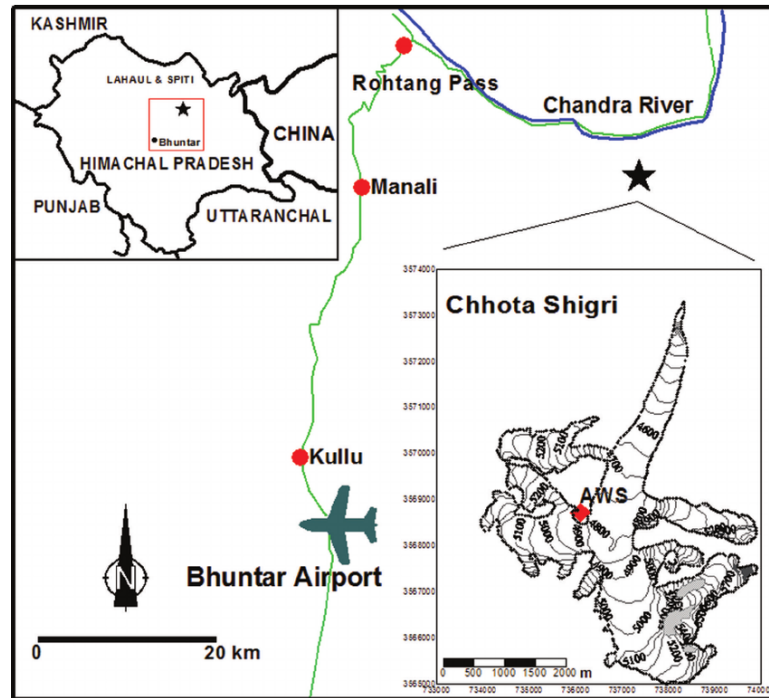


Figure 6: Location map of Chhota Shigri glacier and its surroundings.

Roads are shown in green, river in blue and Chhota Shigri glacier as a star. The upper left inset shows a map of Himachal Pradesh, India, with the location of the Bhuntar Observatory and glacier (star) indicated in the box. The lower right inset is a map of Chhota Shigri glacier with the location of the AWS (red diamond). The map coordinates are in the UTM 43 (north) World Geodetic System 1984 (WGS84) reference system.

Climate is the most important factor that influences glacier dynamics. This glacier is influenced by two atmospheric circulation systems: the Northern Hemisphere mid-latitude westerlies during winter (January–April) and the Indian summer monsoon during summer (July–September) and [14]. It is located in the monsoon–arid transition zone and it feeds Chandra River, one of the tributaries of the Indus River system. The climate of Chhota Shigri and its adjoining area is wet and cool. In the Chandra river valley because of the leeward effect of the main ridge is drier than the southern slopes of the Pir Panjal range. The main ridge is mostly oriented WE, hence preventing part of the monsoon flux from reaching the valley [13]. The lower reaches of the Chhota Shigri glacier are in the dry cold valley zone while the upper accumulation zone experiences occasional precipitation, mostly in the form of snow, sometimes rain drizzle. The higher reaches had a humidity greater than 65%. The yearly precipitation on the glacier is in the range of 150-200 *cm* of snow [35]. This snout of the glacier is well defined, lying in a narrow valley and producing a single

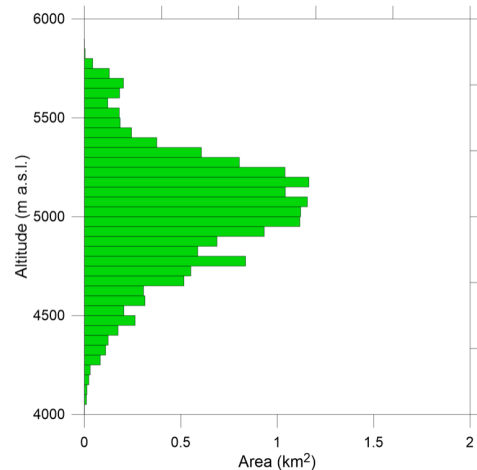


Figure 7: Hypsometry of Chhota Shigri glacier showing 50 m elevation bands

proglacial stream. This glacier is likely to be temperate. The lower ablation area ($<4400\text{ m a.s.l.}$) is covered by debris representing 3.4% of the total surface area [44]. The debris layer is heterogeneous in nature, with silts measuring a few millimeters to big boulders sometimes exceeding a few meters.

<i>Catchment characteristics</i>	Azam et al., 2019 [4]
Latitude	32.28° N
Longitude	77.58° E
Max. Elevation	6263 m asl
Catchment outlet	3840 m asl
Total glacierized area	16.1 km^2
<i>Chhota Shigri Glacier characteristics</i>	
Glacier area	15.5 km^2 (in 2014)
Glacier length	9 km
Snout position	4172 m asl
Mean orientation	North
Maximum elevation	5830 m asl

Table 1: Geographical and topographical characteristics of Chhota Shigri glacier

3 Methodology

3.1 Data Acquisition

The data required for the running of the model included hypsometry of the glacier and meteorological data obtained from The European Centre for Medium-Range Weather Forecasts ECMWF. The ECMWF is an independent intergovernmental organisation supported by most of the nations of Europe and is based at Shinfield Park, Reading, United Kingdom. ERA 5 is the latest dataset provided by ECMWF, known to be the best so far.

3.1.1 ERA 5

The data output from ERA5 is reanalysis data which is obtained from different weather observation stations and satellite data, which is made into data of regular time interval from 1979 to present. The variables are available for two types of data -

1. Single level
2. Pressure level

These data types are available with a resolution of $0.25^{\circ} * 0.25^{\circ}$ for normal variables and $0.5^{\circ} * 0.5^{\circ}$ degree for mean, average variables.

Single level- These data include those data which are independent of the height at which they are taken. For example precipitation, solar radiation, thermal radiation, etc.

Pressure levels- These data include those quantities which vary along the elevation. For example temperature, relative humidity, wind speed, etc. The acquisition of the data was done by running a code in the toolbox of copernicus website specifying the variable, years (maximum limit for

downloading in one go was 12 years, but for the ease of the process we downloaded the variables for sets of six years), area grid (that included the glacier), pressure level (elevation of the glacier at Automatic Weather Station (AWS) explained in the next section), etc. The data obtained was then converted into excel sheet using ArcGIS by changing NetCDF to tables and tables to excel. The files were extracted for the closest four co-ordinates to the glacier i.e. $32.25^{\circ}N$, $32.5^{\circ}N$, $77.5^{\circ}E$, $77.75^{\circ}E$. The excel sheet was made for 6 years set and had to be clubbed together to make a single file from 1979-2019 for each coordinate. The data for the exact location of field data was done using inverse weighted distance method.

$$A_{aws} = \frac{\sum \frac{A_i}{d_i}}{\sum \frac{1}{d_i}} \quad (1)$$

Where A_i 's are the data from the coordinates available from ERA5 and d_i 's are their respective distances from the AWS. Direct extraction of data using ArcGIS at the required AWS location was also an option but on closer analysis it was found that inverse distance formula gives better results on comparison. This might be because ArcGIS takes into account all the grid points to interpolate for the required location because of which the accuracy of the output decreases. Now the data is ready for bias correction.

3.1.2 Automatic Weather Station

Two Automatic Weather Station (AWS's) are installed at the glaciers. AWS 1 on glacier surface at 4663 *m.a.s.l.* and AWS 2 on glacier-side moraine at 4863 *ma.s.l.*. These weather stations are like an automated facility, either on land or sea with equipment and various instruments and sensors to measure atmospheric conditions which can be used in the forecast, to study weather and climate. Climatic variables like temperature, wind speed and direction, radiation, and more such variables can be measured. Details of the sensor along with their sensitivity is given in Table 2 along with the variables examined. Data from AWS 1 is used for bias correction, and data from AWS2 is used to compare the model output. Further details will be discussed in the next section.

3.2 Data Analysis

3.2.1 Bias correction

Global Climate Models (GCM's) have been a vital source of information and data for the construction of any climate scenario. These climate output models are known to have biases. These GCM's provide bias at all scales be it local or global, this limits their application in the study of various climatic scenarios as it leads to erroneous analysis and also induces a range of uncertainties and inaccuracies in the future state of climate projected by these models. Now, Regional climate models aim to provide better dynamically downscaled information generated by GCM's. In the recent past, the availability of regional climate model (RCM) simulations has increased substantially. However, they still present sizable bias like their coarser counterparts. These systematic error (bias) may be due to the limited spatial resolution, numerical scheme, simplified thermodynamic or physics processes, regional geographical attributes etc.

To bias correct or not? Is also a dubious question, it is debated in the scientific community [19] [25] [33]. Data output directly from the climate model could be used, but for impact studies these data will larger biases for *e.g.* Temperature can be consistently too high, model does an incorrect simulation of monsoon as in rain may start early or late, rainfall may be too high or low, or the

Variable	Symbol(unit)	Sensor	Initial Height(m)	Stated Accuracy
AWS 1				
Air temperature	$T_{air}(^{\circ}C)$	Campbell HMP155	0.8&2.5	± 0.1 at $0^{\circ}C$
Relative humidity	$RH(\%)$	Campbell HMP155	0.8&2.5	$\pm 1\%$ at $15^{\circ}C$
Wind speed	$u (ms^{-1})$	A100LK, Vector Inst.	0.8&2.5	± 0.1 upto $10ms^{-1}$
Wind direction	$WD (^{\circ})$	W200P, Vector Inst.	2.5	$\pm 2^{\circ}$
Incoming shortwave	$SWI, (Wm^{-2})$	Kipp&Zonen CNR-4	1.8	$\pm 10\%$ day total
Outgoing shortwave	$SWO, (Wm^{-2})$	Kipp&Zonen CNR-4	1.8	$\pm 10\%$ day total
Incoming longwave	$LWI, (Wm^{-2})$	Kipp&Zonen CNR-4	1.8	$\pm 10\%$ day total
Outgoing longwave	$LWO, (Wm^{-2})$	Kipp&Zonen CNR-4	1.8	$\pm 10\%$ day total
Air pressure	$P_{air} (hPa)$	Young 61302V	1	$\pm 0.3hPa$
Accumulation/Ablation	SR50A (m)	Campbell SR50A	1.6	$\pm 0.1m$
AWS 2				
Air temperature	$T_{air}(^{\circ}C)$	Campbell H3-S3-XT	1.5	± 0.1 at $0^{\circ}C$
Relative humidity	$RH(\%)$	Campbell H3-S3-XT	1.5	$\pm 1.5\%$ at $23^{\circ}C$
Wind speed	$u (ms^{-1})$	Campbell 05103-10-L	3.0	$\pm 0.3ms^{-1}$
Incoming shortwave	$SWI, (Wm^{-2})$	Kipp&Zonen CNR-1	2.5	$\pm 10\%$ day total
Incoming longwave	$LWI, (Wm^{-2})$	Kipp&Zonen CNR-1	2.5	$\pm 10\%$ day total
Precipitation(base camp)	(mm)	Geonor T-200B	1.7(inlet)	$\pm 0.6mm$

Table 2: Measurement specification for Automatic Weather Station on Chhota Shigri AWS 1 located at 4760 m a.s.l. on the mid ablation zone of Chhota Shigri Glacier. AWS 2 located on a morain at 4863 m a.s.l. and the precipitation gauge installed at base camp at 3850 m a.s.l. [1]

model might overestimate the number of days with precipitation or might underestimate the extreme values. Hence, the post processing (such as the removal of bias) of raw output from climate models is important before we use them to study or project any climatic scenario, so that they are a better fit. For bias correction data which is established to be accurate or data acquired directly from field is used. The basic idea behind Bias correction is depicted in the diagram below. Here

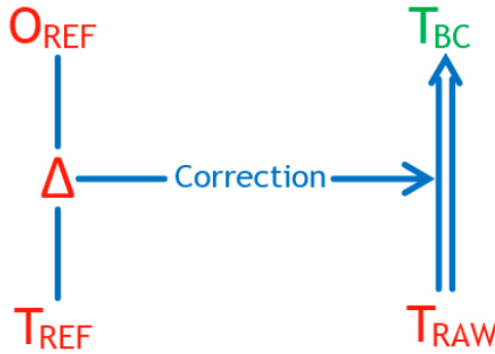


Figure 8: Bias Correction

a relation between the historic reference data between the model output(T_{REF}) and the observed data(O_{REF}) is established using which raw data(T_{RAW}) is corrected (T_{BC}). There are several bias methods available and some methods are more suited to particular variable than the other, this mainly depends on the distribution of data for that variable. Therefore, before using a particular

bias technique the raw data must be properly analysed so that the correct bias method may be used. Randomly using any method would induce further bias rather than correcting the bias. Various methods used for bias correction in this study are listed as follows:

1. Delta method
2. Factor method
3. Linear scaling method
4. Variance scaling method
5. Quantile Mapping

Delta Method

This method is mainly used when the subject variable follows a similar trend with the observed data with a constant bias. The subject variable which is to be corrected is shifted towards the observed data using the difference (delta). This delta is then used to bias correct the whole dataset for overall period

$$\delta = T_{obs} - P_{obs}$$

$$P_{corr} = P_{raw} + \delta$$

Here delta (δ) is calculated using the difference between the observed data (T_{obs}) and the model output (P_{obs}) for the same period. This delta established is used to correct the raw output (P_{raw}). This method is generally applied to variables like temperature.

Factor Method

This method has a similar concept to the above described delta method but unlike delta method we develop a factor or ratio which relates the subject variable and the observed data. This is used for variables like wind speed. Net Shortwave is biased using this method. Figure shows the bias correction of net shortwave. Here factor developed using the ratio is used to correct the raw data.

$$Factor = \frac{T_{obs}}{P_{obs}}$$

$$P_{corr} = Factor * P_{raw}$$

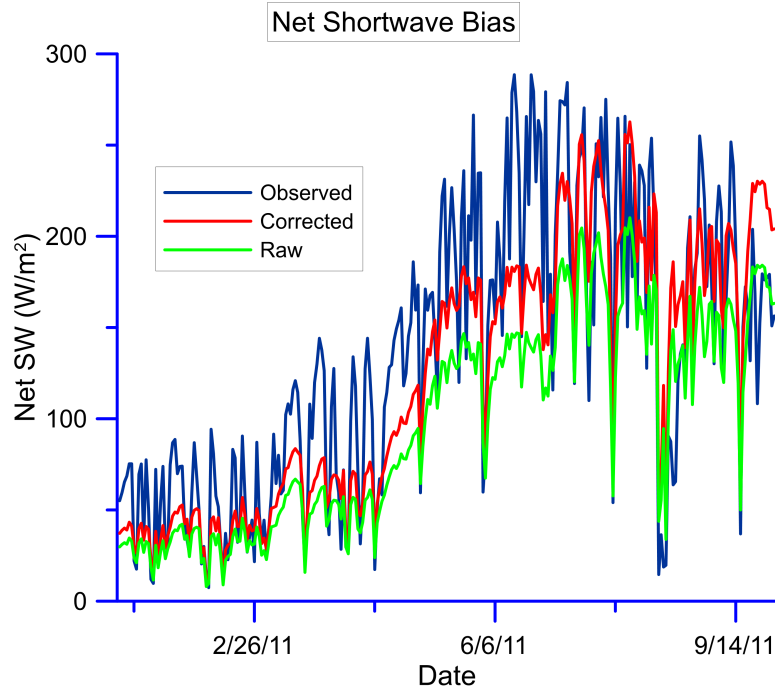


Figure 9: Bias Correction of Net Shortwave

Linear Scaling

The linear scaling method or simply the scaling method adjusts the bias in the model by attempting for an exact match between the monthly mean values of the observed data and that of the subject data which is to be corrected. Using this monthly relation daily values are corrected [16] [20].

$$P_{corr,m,d} = P_{raw,m,d} * \frac{\mu(P_{obs,m})}{\mu(P_{raw,m})}$$

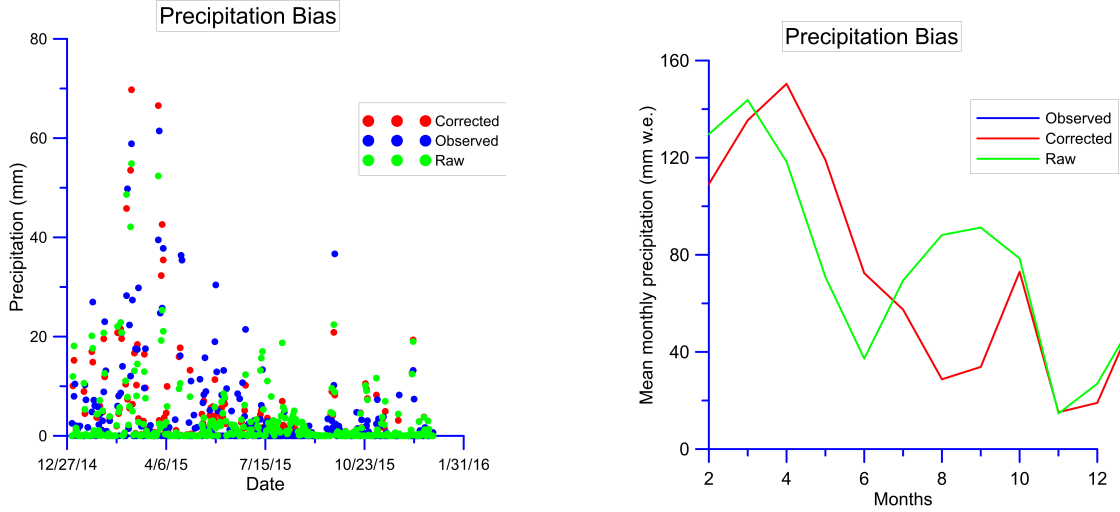
$$T_{corr,m,d} = T_{raw,m,d} + \mu(T_{obs,m}) - \mu(T_{raw,m})$$

Here $P_{corr,m,d}$, $T_{corr,m,d}$ and $P_{raw,m,d}$, $T_{raw,m,d}$ are the corrected model daily value where m and d denote the month and the date respectively. $\mu(P_{obs,m})$, $\mu(T_{obs,m})$ and $\mu(P_{raw,m})$, $\mu(T_{raw,m})$ are the monthly mean of the observed and model data respectively.

The advantage of this method is that it is easy to use and require modest data. This method is a step up when compared to Delta method and Factor method discussed above as it also takes into account the inter-monthly variation of the variable into account. Variables like precipitation and temperature are corrected using this method.

Variance Scaling

The variance scaling method is another step up from the Linear scaling method, unlike the linear scaling method which was only able to correct the mean of the subject variable variance scaling is capable of correcting the mean as well as the variance of the subject. The mean corrected results instituted by the Linear scaling approach are further normalized upon a monthly basis to a zero



(a) Scatter plot showing daily precipitation bias correction (b) Monthly mean of Bias corrected precipitation

Figure 10: Bias Correction of Precipitation

mean [32]. Let $T_{corr,m,d}$ as corrected in the Linear scaling method discussed in the previous section be denoted by $T_{LS,m,d}$. Then a normalized series $T'_{m,d}$ is defined to correct the historical data as:

$$T'_{m,d} = T_{LS,m,d} - \mu(T_{LS,m,d})$$

In the next step the standard deviation ($\sigma'_{m,d}$) of the normalized series is corrected using the ratio of the observed standard deviation monthly ($\sigma_m(T_{obs,m,d})$) and the normalized series standard deviation monthly ($\sigma_m(T'_{m,d})$) as demonstrated:

$$\sigma'_{m,d} = T'_{m,d} * \frac{\sigma_m(T_{obs,m,d})}{\sigma_m(T'_{m,d})}$$

In the final step, the corrected value is calculated using the mean and standard deviation calculated as :

$$T_{corr,m,d} = \sigma'_{m,d} + \mu(T_{LS,m,d})$$

Figure shows the the bias correction of surface temperature using variance scaling.

Quantile Mapping

Quantile Mapping is an advanced bias technique which is capable of correcting all possible distributions of the variable . This is a non parametric bias correction method. This approach originates from empirical transformation [42]. The adjustment of precipitation using Quantile mapping can be expressed in terms of the empirical CDF ($ecdf$) and its inverse ($ecdf^{-1}$) [20].

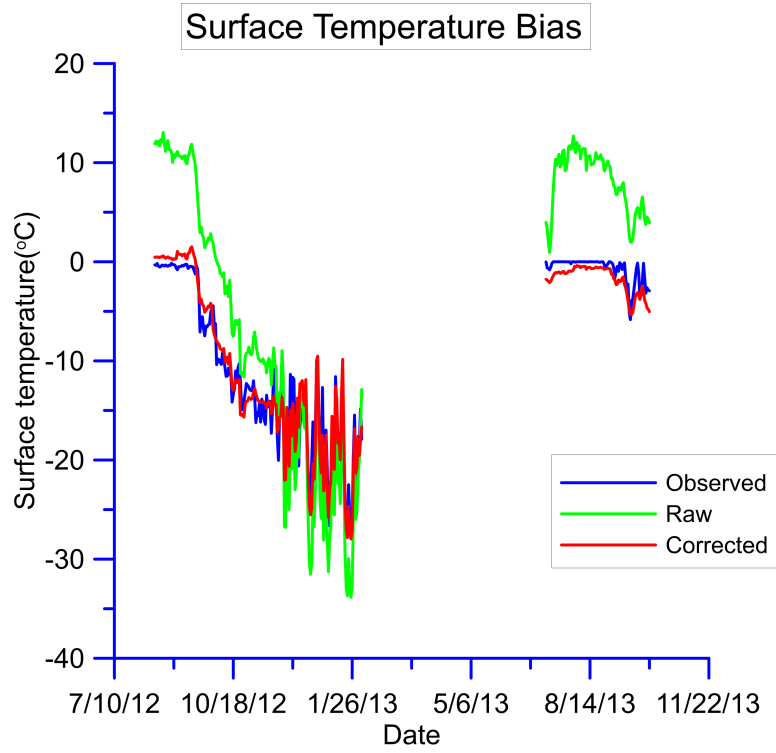


Figure 11: Bias Correction of Surface Temperature

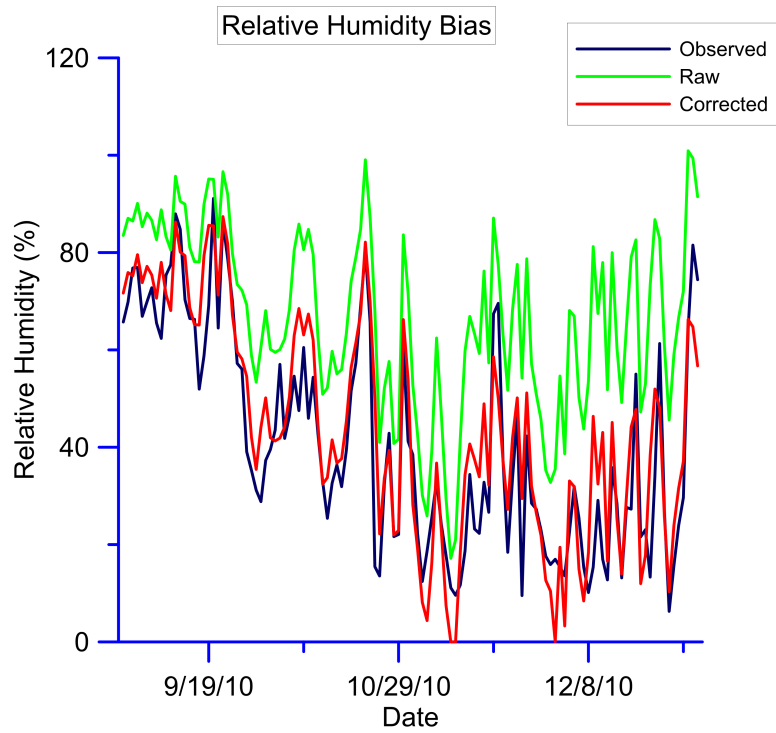


Figure 12: Bias Correction of Relative Humidity

4 Mass Balance Model

4.1 Glacier Wide Mass Balance

The Glacier wide mass balance (B_z) can be calculated using the given formula [41][23] :

$$B_z = \frac{A_z b_z}{A_z}, \quad (2)$$

where, A_z and b_z are the glacier area and the mass balance at 50 m elevation band respectively. The Chhota Shigri glacier was divided into 43 bands of 50 m each. The lowest being 4075 m increasing upto 6175 m.

4.2 Point Mass Balance

Mass Balance (b_z) at an elevation band is calculated as the difference between the accumulation (Acc) and ablation ($melt$).

$$b_z = Acc - Abl, \quad (3)$$

4.2.1 Accumulation

Accumulation term is calculated using the sum of the solid precipitation (P_s), and the Refreeze rate (R_F) as :

$$Acc = P_s + R_F \quad (4)$$

As precipitation takes place mainly during the summer monsoon season in this region which is majorly in the form of rain, phase of precipitation plays a major role in this model. Phase of precipitation is considered to be dependent on the temperature of air as:

$$P_s = P_p \quad T_a < 0^\circ C,$$

$$P_s = 0 \quad T_a > 0^\circ C$$

4.2.2 Ablation

Ablation term includes surface melt, and sublimation and re-sublimation and is calculated as :

$$Abl = melt + R_s \quad (5)$$

Hence, the final formula for the point mass balance ($m.w.e.$) is given as :

$$b_z = \frac{(P_s + R_F) - (melt + R_s)}{\rho_w} \quad (6)$$

where, P_s is the solid precipitation rate ($mm \text{ w.e.} d^{-1}$), (R_s) is the sublimation re-sublimation rate ($mm \text{ w.e.} d^{-1}$), R_F is the refreeze rate ($mm \text{ w.e.} d^{-1}$) and ρ_w is the density of water (1000 kg m^{-2}).

4.3 Melt

The melt is calculated using the heat of melting (Q_m) and the latent heat of melting (l_m). This model was previously discussed in (Fujita and Ageta, 2000 [23] ; Fujita and Sakai, 2014[22]). The heat of melting (Q_m) is defined as follows :

$$Q_m = H_{SR} + H_{LR} - \varepsilon\sigma(T_S + 273.14)^4 + H_S + H_L, \quad (7)$$

where, the heat of melting in the glacier (Q_m, Wm^{-2}) is a function of the net shortwave radiation ($H_{SR} Wm^{-2}$), longwave radiation (H_{LR}, Wm^{-2}), emissivity (ε , dimensionless), Stefan Boltzmann constant ($\sigma, 5.67 * 10^{-8} Wm^{-2}K^{-4}$), surface temperature ($T_S, ^\circ C$), sensible heat flux (H_S, Wm^{-2}), and the latent heat flux (H_L, Wm^{-2}). All components are positive when fluxes directed downwards towards the surface. The heat of melt calculated using the above mentioned formula will only contribute in melting when the surface temperature is above a certain threshold, below this temperature the energy will not be able to change the phase of ice, therefore melt value is calculated as :

$$\begin{aligned} melt &= 0 & T_s < T_o \\ melt &= \frac{Q_m}{l_m} & T_s > T_o \end{aligned}$$

This threshold temperature (T_o) is considered to be $-0.5^\circ C$. Here l_m is the latent heat of fusion of ice ($3.33 * 10^5 Jkg^{-1}$).

4.3.1 Latent and Sensible Heat Flux

Turbulent Latent and Sensible heat fluxes are calculated by the bulk method (Fujita and Ageta, 2000 [23]) :

$$H_S = c_a \rho_a C U (T_a - T_s), \quad (8)$$

$$H_L = l_e \rho_a C U [rhq(T_a) - q(T_s)], \quad (9)$$

where, c_a is the Specific heat of air ($1006 Jkg^{-1}K^{-1}$), l_e is the Latent heat for evaporation ($2.50 * 10^6 Jkg^{-1}$), ρ_a is the Density of air, C is the Bulk coefficient for sensible and latent heat (0.002), U is the Wind speed (ms^{-1}), rh is the Relative humidity, T_a and T_s are the temperature of air and surface respectively (K), $q(T_a)$ and $q(T_s)$ are the Saturated specific humidity at air and surface temperature respectively.

The saturated specific humidity at a temperature T is calculated as :

$$q(T) = 0.622 \frac{e^*}{P}, \quad (10)$$

$$e^* = 0.611 \exp\left(\frac{17.3T}{T + 237.2}\right), \quad (11)$$

where e^* is the Saturation vapour pressure (kPa) and T is the temperature ($^\circ C$).

4.3.2 Density of Air

The density of air (ρ_a) is calculated using the ideal gas equation, expressed as a function of pressure and temperature:

$$\rho_a = \frac{P}{R_{specific} T} \quad (12)$$

where, P is the absolute pressure (Pa), T is the absolute temperature (K) and $R_{specific}$ is the specific gas constant for dry air ($287.058 Jkg^{-1}K^{-1}$).

4.3.3 Surface Temperature

Stefan- Boltzmann equation is employed to calculate the surface temperature using longwave radiation which states that 'The thermal energy radiated by a blackbody radiator per second per unit area(ϕ) is proportional to the fourth power of the absolute temperature(T) and is given by' :

$$\phi = \sigma T^4 \quad (13)$$

where, σ is the stefan boltzmann constant ($\sigma, 5.67 * 10^{-8} Wm^{-2}K^{-4}$).

The surface temperature for various bands is calculated as [23] :

$$T_s = T_a + \frac{H_{SR} + \epsilon H_{LR} - \epsilon \sigma (T_a + 273.2)^4 - l_e \rho_a C U (1 - rh) q(T_a)}{4\epsilon \sigma (T_a + 273.2)^3 + (\frac{dq}{dT_a} l_e + c_a) \rho_a C U} \quad (14)$$

4.4 Refreeze Rate

It has been pointed out that the amount of superimposed ice formed at the ice surface also has some impact on the mass balance of the glacier [5]. The thickness of superimposed ice is calculated as [48] :

$$R_F = -0.69\theta_{14} + 0.0096, \quad (15)$$

where θ_{14} is the ice temperature ($^{\circ}C$) at 14 m depth which is assumed equal to the mean annual air temperature [48].

4.5 Sublimation and Re-sublimation

Sublimation is the process of conversion of a substance from solid to gas without it converting to liquid. The sublimation and re-sublimation hinders the melt (ablation) and is therefore subtracted from it. The sublimation/re-sublimation is calculated using the latent heat of sublimation using the following formula:

$$R_s = \frac{H_L}{l_s}, \quad (16)$$

where H_L is the latent heat flux and l_s is the latent heat of sublimation equals $26400 Jkg^{-1}$.

5 Future Mass Balance

Global climatic projections are used for the prediction of future climatic conditions. These global climatic projections are climate model simulations developed in an effort coordinated by the World Climate Research Program (WCRP) where multiple independent climate research centers have contributed. These have been assessed by the Intergovernmental Panel on Climate Change (IPCC).

The Climate Model Intercomparison Project (CMIP)

Various climate models with an agreed set of inputs from all around the world, various research institutes or national meteorological centres contribute in the CMIP process. These modelling centers produce set of standardised output, these when combined these produce a multi-model dataset. The models so developed can be shared in the international community and various modelling centres and results can be compared.

Representative Concentration Pathway

Representative Concentration Pathway (RCP) are greenhouse gas concentrations adopted by the Intergovernmental Panel on Climate Change IPCC for its fifth Assessment Report (AR5) in 2014. These are concentration values and not emissions. This was preceded by the Special Report on Emissions Scenarios (SRES) projections which were published in 2000. Four pathways namely RCP2.6, RCP4.5, RCP6, and RCP8.5 have been selected for climate modeling and research. These climate scenarios are described considering possible greenhouse gases emitted in the upcoming years. The four RCPs, are labelled after a possible range of radiative forcing values in the year 2100 (2.6, 4.5, 6.0, and 8.5 Wm^{-2} , respectively). We have calculated the future glacier mass balance of Chhota Shigri glacier for RCP4.5 and RCP8.5, RCP 8.5 being extreme condition and RCP4.5 being a more realistic future scenario.

CNRM-CM5

The model used out of all the CMIP5 models for the future projections is the CNRM-CM5 (CNRM-CERFACS, France). This is the new version of the general circulation model CNRM-CM. CNRM-CM5 has been developed jointly by CNRM-GAME (Centre National de Recherches Meteorologiques-Groupe d'etudes de l' Atmosphere Meteorologique and Cerfacs (Centre Europeen de Recherche et de Formation Avancee) in order to contribute to phase 5 of the Coupled Model Intercomparison Project (CMIP5).

Some major improvements since the CMIP3 are as follows[46]:

- Horizontal resolution has been increased from 2.8° to 1.4° in the atmosphere and from 2° to 1° in the ocean.
- Radiation scheme has been revised, tropospheric and stratospheric aerosols treatments has been improved.
- For the atmospheric component the dynamical core has been revised.
- Special care has been given to ensure mass/water conservation in the atmospheric component.

- The atmospheric model through the SURFEX platform has been used to externalised The land surface scheme ISBA, this includes ew developments such as a parameterization of sub-grid hydrology and a new freezing scheme.
- The ocean model OPA8.0 version used in the CMIP3 version of CNRM-CM has been improved to the new state-of-the-art version of NEMO, which has greatly progressed since the OPA8.0
- Particular attention to avoid energy loss and spurious drifts has been incorporated between different components through OASIS.

The model used a similar approach but instead of using daily values we are using monthly averages and calculating the Mass Balance. Here we are not considering the snout retreat which can be a major factor in the future as the loss of the glaciers is very large. The model variables are biased with the same factors as in the past mass balancing. The extrapolation of the point mass balance to the glacier wide mass balance is done using lapse rate, precipitation gradient from field data of the past, whereas the wind speed gradient and surface temperature gradient is found out in the past mass balancing and used in this model.

6 Results and Discussion

The extrapolation of the data was done for different variable after the bias correction of the data for different elevation bands with 50 m increments from 4075 m a.s.l. to 6175 m a.s.l. and pressure level from 61040.15 Pa to 46059.82 Pa. Precipitation gradient and lapse rate (available from 1969-daily values) were taken from field data. Wind speed calculation for different bands was done using different change rates for bands higher than 5525 m a.s.l., 4875 m a.s.l., 4175 m a.s.l. and lower than 4175 m a.s.l. using values obtained for different pressure levels from ERA 5. Relative humidity was used directly with bias at 450, 500, 550, 600, and 650 *hPa*, and interpolated for the exact *hPa* of the bands using the linear interpolation of the closest two values. The annual mass balance values (hydrological year) for 1980 to 2018 are -0.55 ± 0.56 *m.w.e.a⁻¹* (value along with the standard deviation). Mass balance annual values are calculated for Hydrological years which starts from 1st October till the 30th of September next year.

6.1 Annual Mass Balance

6.1.1 Annual hydrologic mass balance since 1980

The 1980–2018 glacier-wide modelled Mass Balance are displayed in Figure 13 The model was run for 1 January 1979 to 1 April 2019 with daily values of mass balance 3.437 *mmw.e.* ranging from 131.674 *mmw.e.* to -54.25 *mm.w.e.* with 52.24% values as negative. In the recent years annual mass balance has been mostly negative except for the year 2014 and 2015 with values 0.25 *m.w.e* and $+0.84$ *m.w.e* respectively. Mass balance (hydrological year) in the last 10 years has been most negative for the year 2018 with a mass balance value of -1.01 *m.w.e* . An average mass balance of -0.29 ± 0.715 *m.w.e.a⁻¹* for the years 2010 to 2018. The previous decadal values are -0.86 ± 0.321 *m.w.e.a⁻¹* for 2000-2009, -0.64 ± 0.439 *mw.e.a⁻¹* for 1990-1999, -0.39 ± 0.620 *m.w.e.a⁻¹* for 1980-1989.

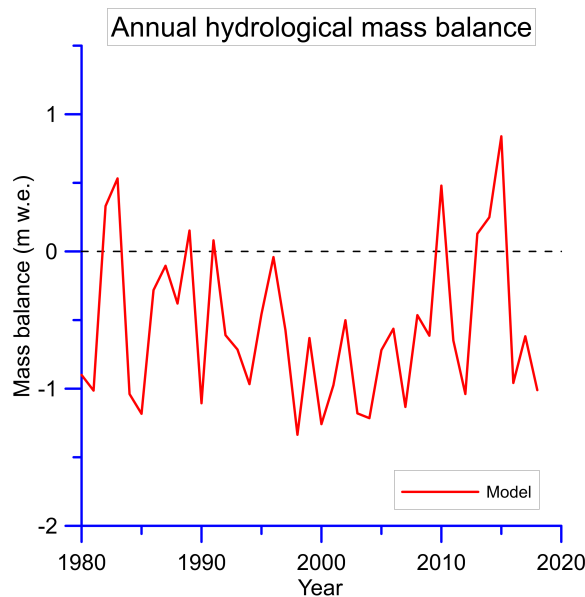


Figure 13: Annual hydrologic mass balance since 1980

6.1.2 Seasonal Mass Balance

The mass balance for different season show similar trends than what is expected, the summer season (May-September) show most negative values as the average temp and radiation on the glacier surface is more as compared to other seasons resulting in lower solid precipitation values with values $-0.19 \pm 0.09 \text{ mw.e.a}^{-1}$ per month, and the winter period (October-April) with the highest positive values as the surface temperature is more negative and the days are colder resulting in positive mass balance $0.10 \pm 0.03 \text{ mw.e.a}^{-1}$ per month. The results of the model follow the seasonality of the glacier.

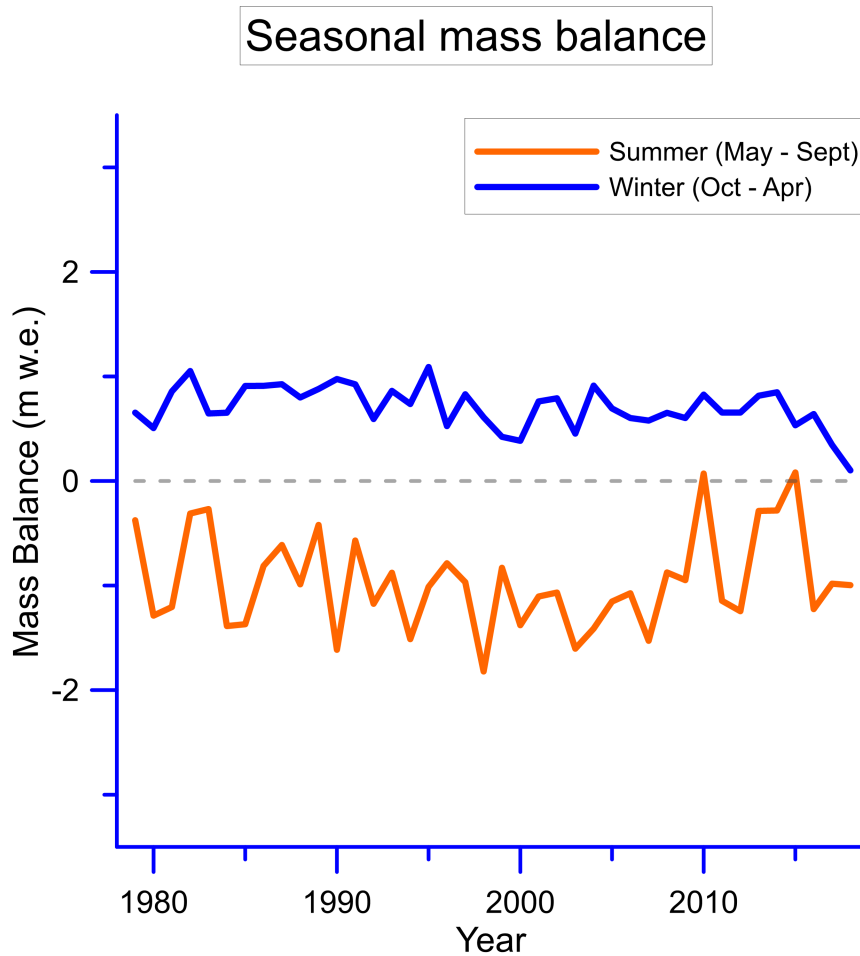


Figure 14: Seasonal Mass Balance

6.2 Model performance

Figure15 gives a graphical comparison between the model and (Azam et al. [2]). (Azam et al. [2]) has used field data to calculate the mass balance. A coefficient of determination of 0.769 is obtained. This shows a close relation between the two results. Figure16 shows comparison from various available mass balance for various years. Here we have incorporated geodetic as well as field calculated mass balance values.

Type	Year	Model	Reference	Source
Geodetic	1999-2011	-0.72 ± 0.46	-0.24 ± 0.10	[34]
Geodetic	1999-2004	-0.96 ± 0.32	-0.70	[11]
Geodetic	2005-2014	-0.43 ± 0.54	-0.23 ± 0.28	[15]
Geodetic	2005-2014	-0.43 ± 0.54	-0.27 ± 0.13	[15]
Geodetic	1999-2010	-0.73 ± 0.31	-0.44 ± 0.16	[44]
Field	2012-2014	-0.22 ± 0.71	-0.42 ± 0.40	[2]
Field	2002-2012	-0.56 ± 0.55	-0.59 ± 0.40	[2]

Table 3: Table showing comparison of modelled mass balance with available mass balances ($mw.e.a^{-1}$)

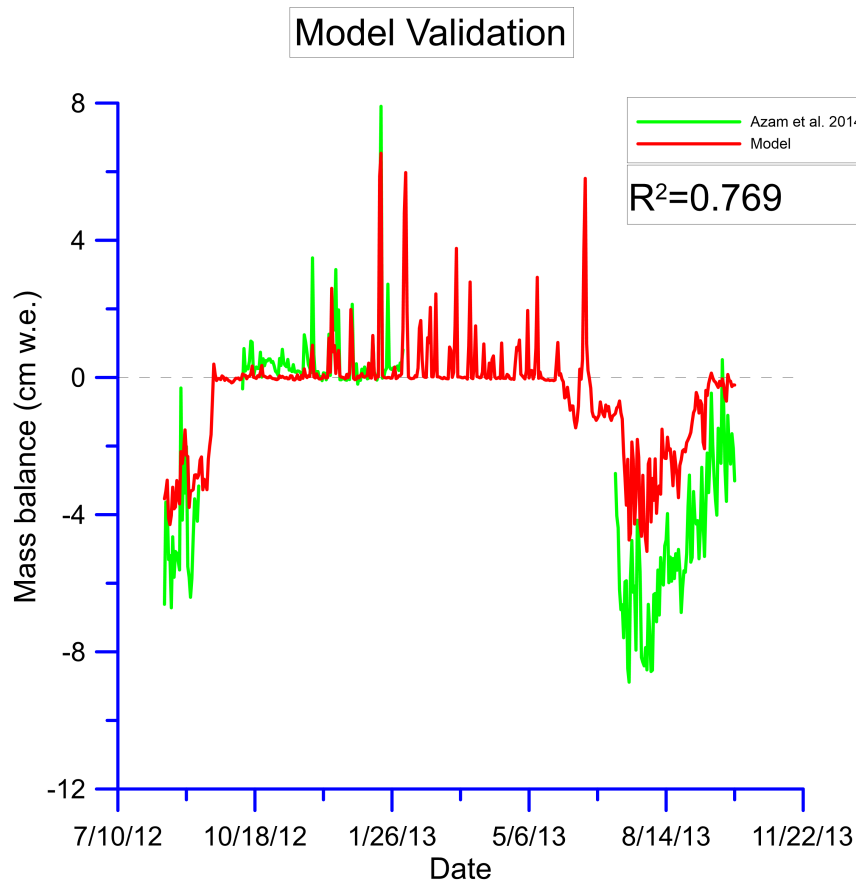


Figure 15: Mass Balance comparison with field data

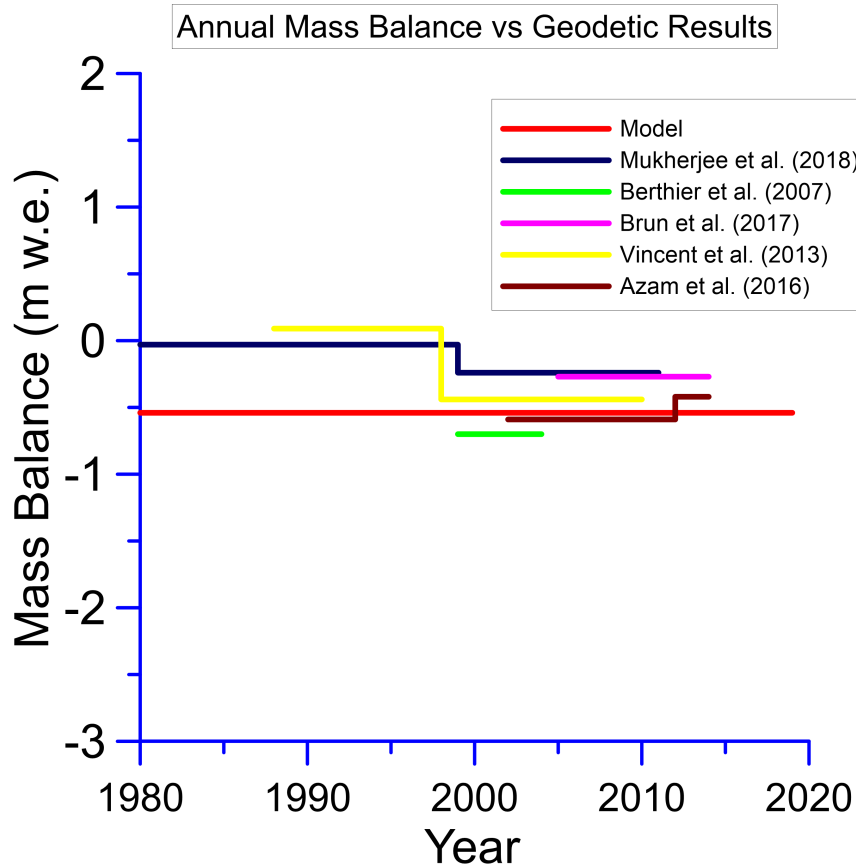


Figure 16: Mass Balance comparison with geodetic data

6.3 Mass Balance as a function of Altitude

The mass balance of different bands follow strictly increasing trend with more accumulation (positive mass balance values) at higher elevations and more ablation (negative mass balance values) in the lower regions of the glacier. The equilibrium line altitude (ELA) lies approximately in between 5000 to 5500 m a.s.l. for the years 2010-2017. The graphs shows that the lower regions of the glaciers are losing mass at a faster pace resulting in overall mass loss for the glacier. The method used for the calculation of the mass balance uses gradients for various variables that are used for calculating different parameters of the mass balance. We see that for overall negative mass balances the ablation zone is more than the accumulation zone, the external factors that affect this portions are the increase in temperature of the glaciers and as a result increase in the hot days with lower solid precipitation and more heat of melt.

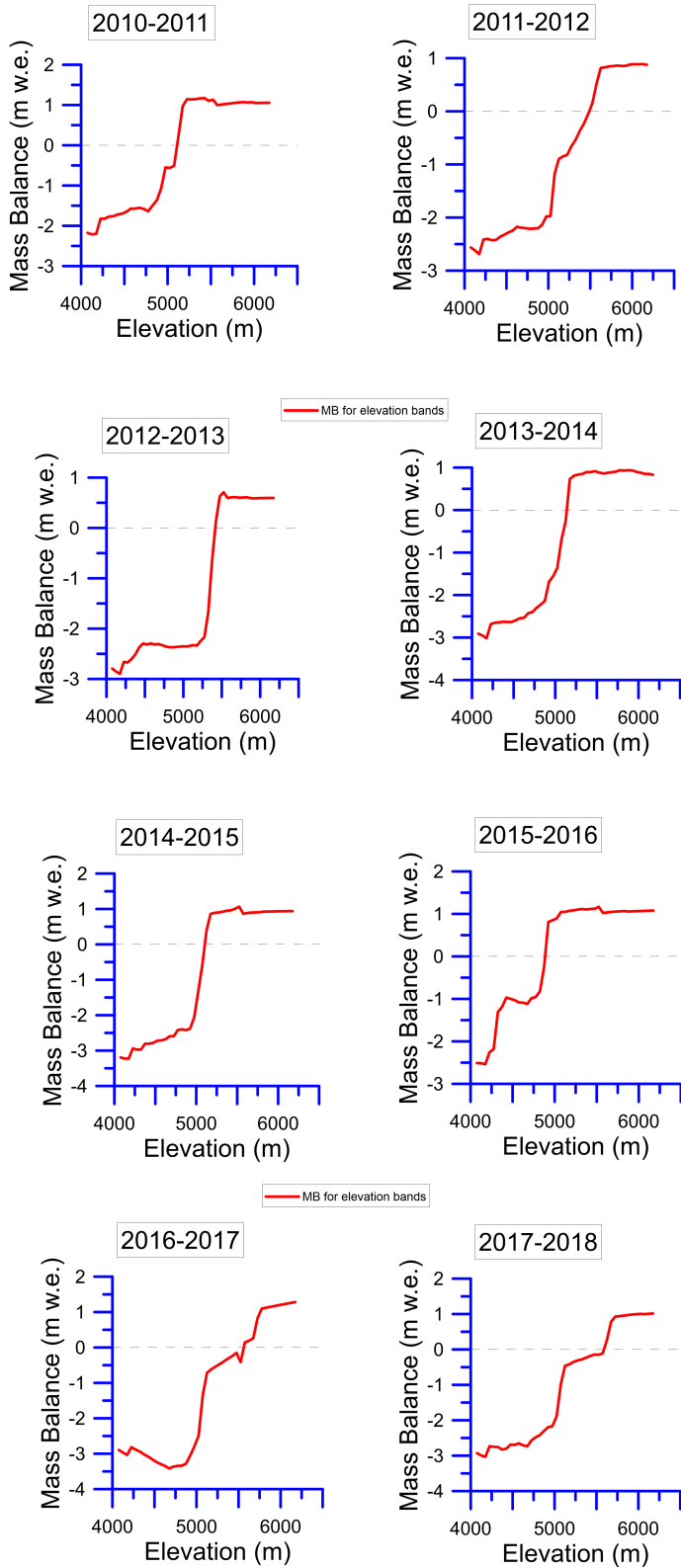


Figure 17: Mass Balance vs elevation 2010-2017

6.4 Future Mass Balance

The future mass balance values for RCP 4.5 are $-6.7 \pm 0.30 \text{ m w.e.a}^{-1}$ with increasing loss of mass in the glacier for the period of 2006-2100. The future mass balance values for RCP 8.5 are $-12.88 \pm 0.57 \text{ m w.e.a}^{-1}$ with increasing loss of mass in the glacier for the period of 2006-2100. The results can be understood as the air temperature is increasing more and more, we can say that the glacier will lose more mass. The results for RCP 8.5 are extreme case which would happen when we are not considering the climate change at all and keep on exploiting the environment at an even higher rate. While at RCP 4.5 although the mass loss is quite large if we try to conserve the glacial systems we might not even have to worry about the increase in loss.

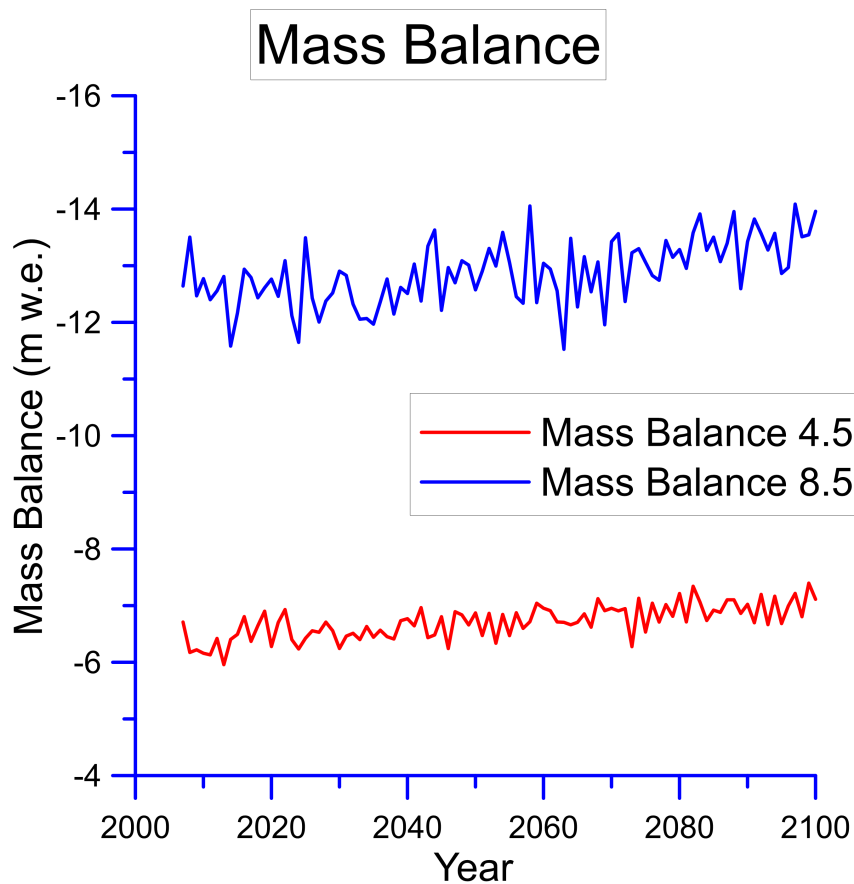


Figure 18: Mass Balance for RCP 4.5 and 8.5 year 2007-2100

7 Conclusion

The model results indicate a steady loss of mass in the glacier of about $-0.56 \pm 0.55 \text{ mw.e.a}^{-1}$, which shows that the glacier is in a state of bad health. There can be various reasons for this loss but one of the major reasons is the rise of the global air temperature with about 0.2 degree celsius rise per decade. The model is a simple approach that can be used for the mass balance of any glacier with the availability of some basic variables, and some field data for bias correction and calibration. Most of the variables available with ERA5 have quite good relations with the field data, incorporating the seasonality and general trend. We tried different datasets for the model but found that ERA5 gives the best output and thus is the best dataset for glaciological modelling available so far. The results of the model show great sensitivity to air and surface temperature, and we cannot possibly control surface temperature but we can try to reduce the increase of the air temperature especially in the regions close to the glaciers.

The future model results have increasing mass loss in the years in the future which might reduce if the glacier orography and removal of bands where mass has been lost are considered (snout retreat). For 4.5 RCP we have an increase of about 0.6 mw.e.a^{-1} in the mass loss in the average of the first decade of the modelling time to the average of the last decade, while for 8.5 RCP we have an increase of about 1 mw.e.a^{-1} in the mass loss in the average of the first decade of the modelling time to the average of the last decade. Future modelling of the glacier can be improved by incorporating glacier dynamics into the model to give better results but the loss of glacier mass is not something that the model depicted wrong, the values might be slightly lower but the glacier would be still losing mass at a deadly rate.

References

- [1] MF Azam, Patrick Wagnon, C Vincent, AL Ramanathan, V Favier, A Mandal, and JG Pottakkal. Processes governing the mass balance of chhota shigri glacier (western himalaya, india) assessed by point-scale surface energy balance measurements. *The Cryosphere*, 8(6):2195–2217, 2014.
- [2] Mohd Farooq Azam, AL Ramanathan, Patrick Wagnon, C Vincent, A Linda, E Berthier, P Sharma, A Mandal, T Angchuk, VB Singh, et al. Meteorological conditions, seasonal and annual mass balances of chhota shigri glacier, western himalaya, india. *Annals of Glaciology*, 57(71):328–338, 2016.
- [3] Mohd Farooq Azam, Patrick Wagnon, Alagappan Ramanathan, Christian Vincent, Parmanand Sharma, Yves Arnaud, Anurag Linda, Jose George Pottakkal, Pierre Chevallier, Virendra Bahadur Singh, et al. From balance to imbalance: a shift in the dynamic behaviour of chhota shigri glacier, western himalaya, india. *Journal of Glaciology*, 58(208):315–324, 2012.
- [4] Mohd Farooq Azam, Patrick Wagnon, Christian Vincent, AL Ramanathan, Naveen Kumar, S Srivastava, JG Pottakkal, and Pierre Chevallier. Snow and ice melt contributions in a highly glacierized catchment of chhota shigri glacier (india) over the last five decades. *Journal of Hydrology*, 574:760–773, 2019.
- [5] Mohd Farooq Azam, Patrick Wagnon, Christian Vincent, Alagappan Ramanathan, Anurag Linda, and Virendra Bahadur Singh. Reconstruction of the annual mass balance of chhota shigri glacier, western himalaya, india, since 1969. *Annals of Glaciology*, 55(66):69–80, 2014.
- [6] David B Bahr, Mark Dyurgerov, and Mark F Meier. Sea-level rise from glaciers and ice caps: A lower bound. *Geophysical Research Letters*, 36(3), 2009.
- [7] Prashant Baral, Rijan B Kayastha, Walter W Immerzeel, Niraj S Pradhananga, Bikas C Bhattarai, Sonika Shahi, Stephan Galos, Claudia Springer, Sharad P Joshi, and Pradeep K Mool. Preliminary results of mass-balance observations of yala glacier and analysis of temperature and precipitation gradients in langtang valley, nepal. *Annals of glaciology*, 55(66):9–14, 2014.
- [8] DI Benn and DJA Evans. *Glaciers and glaciation*. hodder education. London, UK, page 802, 2010.
- [9] Douglas I Benn and Frank Lehmkuhl. Mass balance and equilibrium-line altitudes of glaciers in high-mountain environments. *Quaternary International*, 65:15–29, 2000.
- [10] Keith Benn, Richard J Horne, Daniel J Kontak, Geoffrey S Pignotta, and Neil G Evans. Syn-acadian emplacement model for the south mountain batholith, meguma terrane, nova scotia: Magnetic fabric and structural analyses. *Geological Society of America Bulletin*, 109(10):1279–1293, 1997.
- [11] Etienne Berthier, Yves Arnaud, Rajesh Kumar, Sarfaraz Ahmad, Patrick Wagnon, and Pierre Chevallier. Remote sensing estimates of glacier mass balances in the himachal pradesh (western himalaya, india). *Remote Sensing of Environment*, 108(3):327–338, 2007.

- [12] Tobias Bolch, Anil Kulkarni, Andreas Kääb, Christian Huggel, Frank Paul, J Graham Cogley, Holger Frey, Jeffrey S Kargel, Koji Fujita, Marlene Scheel, et al. The state and fate of himalayan glaciers. *Science*, 336(6079):310–314, 2012.
- [13] Bodo Bookhagen and Douglas W Burbank. Topography, relief, and trmm-derived rainfall variations along the himalaya. *Geophysical Research Letters*, 33(8), 2006.
- [14] Bodo Bookhagen and Douglas W Burbank. Toward a complete himalayan hydrological budget: Spatiotemporal distribution of snowmelt and rainfall and their impact on river discharge. *Journal of Geophysical Research: Earth Surface*, 115(F3), 2010.
- [15] Fanny Brun, Etienne Berthier, Patrick Wagnon, Andreas Kääb, and Désirée Treichler. A spatially resolved estimate of high mountain asia glacier mass balances from 2000 to 2016. *Nature geoscience*, 10(9):668, 2017.
- [16] A Choudhary and AP Dimri. On bias correction of summer monsoon precipitation over india from cordex-sa simulations. *International Journal of Climatology*, 39(3):1388–1403, 2019.
- [17] J Graham Cogley, Jeffrey S Kargel, Georg Kaser, and Cornelis J van der Veen. Tracking the source of glacier misinformation. *Science*, 327(5965):522–522, 2010.
- [18] Mark B Dyurgerov, Mark F Meier, et al. *Glaciers and the changing Earth system: a 2004 snapshot*, volume 58. Institute of Arctic and Alpine Research, University of Colorado Boulder, 2005.
- [19] U Ehret, E Zehe, V Wulfmeyer, K Warrach-Sagi, and J Liebert. Hess opinions” should we apply bias correction to global and regional climate model data?”. *Hydrology and Earth System Sciences*, 16(9):3391–3404, 2012.
- [20] Gonghuan Fang, J Yang, YN Chen, and C Zammit. Comparing bias correction methods in downscaling meteorological variables for a hydrologic impact study in an arid area in china. *Hydrology and Earth System Sciences*, 19(6):2547–2559, 2015.
- [21] P Forster, V Ramaswamy, P Artaxo, T Berntsen, R Betts, DW Fahey, J Haywood, J Lean, DC Lowe, G Myhre, et al. Contribution of working group i to the fourth assessment report of the intergovernmental panel on climate change. *Climate change*, pages 129–234, 2007.
- [22] K Fujita and A Sakai. Modelling runoff from a himalayan debris-covered glacier. *Hydrology and Earth System Sciences*, 18(7):2679–2694, 2014.
- [23] Koji Fujita and Yutaka Ageta. Effect of summer accumulation on glacier mass balance on the tibetan plateau revealed by mass-balance model. *Journal of Glaciology*, 46(153):244–252, 2000.
- [24] Koji Fujita and Takayuki Nuimura. Spatially heterogeneous wastage of himalayan glaciers. *Proceedings of the National Academy of Sciences*, 108(34):14011–14014, 2011.
- [25] Stefan Hagemann, Cui Chen, Jan O Haerter, Jens Heinke, Dieter Gerten, and Claudio Piani. Impact of a statistical bias correction on the projected hydrological changes obtained from three gcms and two hydrology models. *Journal of Hydrometeorology*, 12(4):556–578, 2011.

- [26] T Heid and A Käab. Repeat optical satellite images reveal widespread and long term decrease in land-terminating glacier speeds. *The Cryosphere*, 6(2):467–478, 2012.
- [27] H Hoinkes. *Methoden und Möglichkeiten von Massenhaushaltsstudien auf Gletschern: Ergebnisse der Messreihe Hintereisferner (Ötztaler Alpen) 1953-1968*. Wagner, 1970.
- [28] WW Immerzeel, F Pellicciotti, and MFP Bierkens. Rising river flows throughout the twenty-first century in two himalayan glacierized watersheds. *Nature geoscience*, 6(9):742, 2013.
- [29] MK Kaul and VMK Puri. *Inventory of the Himalayan glaciers: a contribution to the International Hydrological Programme*. Number 34. Geological Survey of India, 1999.
- [30] Owen King, Duncan J Quincey, Jonathan L Carrivick, and Ann V Rowan. Spatial variability in mass loss of glaciers in the everest region, central himalayas, between 2000 and 2015. *The Cryosphere*, 11(1):407–426, 2017.
- [31] Surendar Kumar and DP Dobhal. Climatic effects and bedrock control on rapid fluctuations of chhota shigri glacier, northwest himalaya, india. *Journal of Glaciology*, 43(145):467–472, 1997.
- [32] Min Luo, Tie Liu, Fanhao Meng, Yongchao Duan, Amaury Frankl, Anming Bao, and Philippe De Maeyer. Comparing bias correction methods used in downscaling precipitation and temperature from regional climate models: a case study from the kaidu river basin in western china. *Water*, 10(8):1046, 2018.
- [33] Markus Muerth, B Gauvin St-Denis, S Ricard, JA Velázquez, J Schmid, M Minville, D Caya, D Chaumont, Ralf Ludwig, and R Turcotte. On the need for bias correction in regional climate scenarios to assess climate change impacts on river runoff. *Hydrology and Earth System Sciences Discussions*, pages 10205–10243, 2012.
- [34] Kriti Mukherjee, Atanu Bhattacharya, Tino Pieczonka, Susmita Ghosh, and Tobias Bolch. Glacier mass budget and climate reanalysis data indicate a climatic shift around 2000 in lahaul-spiti, western himalaya. *Climatic change*, 148(1-2):219–233, 2018.
- [35] VN Nijampurkar and DK Rao. Accumulation and flow rates of ice on chhota shigri glacier, central himalaya, using radio-active and stable isotopes. *Journal of Glaciology*, 38(128):43–50, 1992.
- [36] Sandeep Chamling Rai and Aarati Gurung. Raising awareness of the impacts of climate change: Initial steps in shaping policy in nepal. *Mountain Research and Development*, 25(4):316–321, 2005.
- [37] CV Sangewar, SP Shukla, and RK Singh. Inventory of the himalayan glaciers. 2009.
- [38] Christopher A. Scott, Fan Zhang, Aditi Mukherji, Walter Immerzeel, Daanish Mustafa, and Luna Bharati. *Water in the Hindu Kush Himalaya*, pages 257–299. Springer International Publishing, Cham, 2019.
- [39] Sonam Futi Sherpa, Patrick Wagnon, Fanny Brun, Etienne Berthier, Christian Vincent, Yves Lejeune, Yves Arnaud, Rijan Bhakta Kayastha, and Anna Sinisalo. Contrasted surface mass balances of debris-free glaciers observed between the southern and the inner parts of the everest region (2007–15). *Journal of Glaciology*, 63(240):637–651, 2017.

- [40] Thomas F Stocker, Dahe Qin, G-K Plattner, Melinda MB Tignor, Simon K Allen, Judith Boschung, Alexander Nauels, Yu Xia, Vincent Bex, and Pauline M Midgley. Climate change 2013: The physical science basis. contribution of working group i to the fifth assessment report of ipcc the intergovernmental panel on climate change, 2014.
- [41] Sojiro Sunako, Koji Fujita, Akiko Sakai, and RIJAN B KAYASTHA. Mass balance of tram-bau glacier, rolwaling region, nepal himalaya: in-situ observations, long-term reconstruction and mass-balance sensitivity. *Journal of Glaciology*, pages 1–12, 2019.
- [42] Matthias Jakob Themeßl, Andreas Gobiet, and Georg Heinrich. Empirical-statistical down-scaling and error correction of regional climate models and its impact on the climate change signal. *Climatic Change*, 112(2):449–468, 2012.
- [43] Phuntsho Tshering and Koji Fujita. First in situ record of decadal glacier mass balance (2003–2014) from the bhutan himalaya. *Annals of Glaciology*, 57(71):289–294, 2016.
- [44] C Vincent, Al Ramanathan, Patrick Wagnon, DP Dobhal, Anurag Linda, Etienne Berthier, P Sharma, Yves Arnaud, MF Azam, Julie Gardelle, et al. Balanced conditions or slight mass gain of glaciers in the lahaul and spiti region (northern india, himalaya) during the nineties preceded recent mass loss. 2013.
- [45] Christian Vincent, Patrick Wagnon, Joseph Shea, Walter Immerzeel, Philip Kraaijenbrink, Dibas Shrestha, Alvaro Soruco, Yves Arnaud, Fanny Brun, Etienne Berthier, et al. Reduced melt on debris-covered glaciers: investigations from changri nup glacier, nepal. 2016.
- [46] Aurore Voltaire, E Sanchez-Gomez, D Salas y Méliá, B Decharme, Christophe Cassou, S Sénési, Sophie Valcke, I Beau, A Alias, M Chevallier, et al. The cnrm-cm5. 1 global climate model: description and basic evaluation. *Climate Dynamics*, 40(9-10):2091–2121, 2013.
- [47] Patrick Wagnon, Anurag Linda, Yves Arnaud, Rajesh Kumar, Parmanand Sharma, Christian Vincent, Jose George Pottakkal, Etienne Berthier, Alagappan Ramanathan, Syed Iqbal Hasnain, et al. Four years of mass balance on chhota shigri glacier, himachal pradesh, india, a new benchmark glacier in the western himalaya. *Journal of Glaciology*, 53(183):603–611, 2007.
- [48] John Woodward, Martin Sharp, and Anthony Arendt. The influence of superimposed-ice formation on the sensitivity of glacier mass balance to climate change. *Annals of Glaciology*, 24:186–190, 1997.

THE END.